supported by the rate law, however. For rate-limiting transmembrane redox, viologen reduction will be independent of $S_2O_4^{2-}$, yet k_3 shows half-order dependence upon reductant concentration (Figure 6).

It is also evident from product spectra that the k_3 pathway is associated with formation of multimeric viologen radical, as opposed to the predominantly monomeric ions formed by k_1 and k_2 pathways. This reaction involves viologen reduction, i.e., is not merely monomer–multimer equilibration, because absorbance increases are observed over the entire spectral range, including regions where the monomer is more strongly absorbing than multimers,[25] and because simple aggregation–disaggregation equilibration also cannot account for the reaction dependence upon $S_2O_4^{2-}$ concentration.

The intracellular location and structural character of these multimers are presently unknown. One intriguing possibility is that they are organized in a fashion that allows both access by reagents in the external aqueous phase and rapid transmembrane redox, comparable to recently proposed liposome-bound cytochrome c_3[46] and metalloporphyrin[47] dimers, which are described as membrane-traversing electron channels. Aggregation might arise as a consequence of differences in surfactant packing forces on the convex and concave vesicular surfaces; asymmetric binding of tris(2,2′-bipyridine)ruthenium(II) to inner and outer DHP surfaces has recently been proposed based upon optical spectroscopic and equilibrium distribution data.[48] In part to resolve these issues, we are currently characterizing the viologen binding environments by a variety of physical techniques.

Concluding Comments. These studies illustrate the exquisite sensitivity of reaction dynamics in probing environments of vesicle-bound reagents. Even though considerable care was taken to eliminate complications that might arise from microcompartmentation, particle heterogeneity, or surface aggregation of reactants, the kinetics reveals a diversity of viologen binding that is dependent upon subtle structural factors and topographic organization of the particles. Characterization of the molecular organization comprising the kinetically distinct sites may be crucial to understanding transmembrane redox, since the data suggest that this process may occur from only one of the several distinguishable binding domains.

Acknowledgments. Financial support for this research was provided by a grant from the Division of Chemical Sciences, Office of Basic Energy Sciences, U.S. Department of Energy (DE-AC-06-83ER-13111). The digital oscilloscope used in the fast-kinetic studies was obtained through a grant (8522) from the Medical Research Foundation of Oregon. The authors are deeply grateful to these agencies for their program support.

(46) Tabushi, I.; Nishiya, T.; Shimomura, M.; Kunitake, T.; Inokuchi, H.; Tatsuhiko, Y. *J. Am. Chem. Soc.* **1984**, *106*, 219–226.
(47) Yusupov, R. G.; Asanov, A. N.; Khairutdinov, R. F. *Izv. Akad. Nauk SSSR Ser. Khim.* **1985**, 277–282.
(48) Tricot, Y.-M.; Furlong, D. N.; Mau, A. W.-H.; Sasse, W. H. F. *Aust. J. Chem.* **1985**, *38*, 527–535.

Partial Valence Trapping in a Trinuclear Mixed-Valence Iron(III,III,II) Cluster: Vibrational Spectra of $[Fe_3O(OOCCH_3)_6L_3]$ and Related Mixed-Metal Complexes[1]

L. Meesuk, U. A. Jayasooriya, and R. D. Cannon*

Contribution from the School of Chemical Sciences, University of East Anglia, Norwich NR4 7TJ, England. *Received August 11, 1986*

Abstract: Infrared spectra (800–130 cm^{-1}) of the mixed-metal and mixed-valence complexes $[Fe^{III}_2M^{II}O(OOCCH_3)_6L_3]$ (M = Mn, Fe, Co, Ni; L = H_2O, pyridine), and Raman spectra of the aquo-adducts, are reported and assigned by using a variety of isotopic substitutions. It is concluded that in the mixed-valence complexes (M = Fe) the oxidation states are partially localized on the vibrational time scale.

Mixed-valence materials are important for understanding the dynamics of electron-transfer processes,[2] and for this purpose the family of metal complexes of the general formula $[M_3O(OOCR)_6L_3]$ (see Figure 1) is proving to be particularly interesting. The best-known complexes are those containing the $Fe^{III}_2Fe^{II}$ cluster,[3-10] but the range has been extended to include $V^{III}_2V^{II}$,[11] $Cr^{III}_2Cr^{II}$,[12] $Mn^{III}_2Mn^{II}$,[13,14] $Ru^{III}_2Ru^{II}$,[15] $Ir^{IV}_2Ir^{III}$,[16] and, in the case of ruthenium[17] and iridium[18] clusters, several other combinations of oxidation states obtained by electrolytic oxidation and reduction.

With all these compounds, a key question is whether the metal ion triangle is exactly equilateral, with all other corresponding metal–ligand bonds equal (D_{3h} symmetry), or whether one metal

(1) Part VII of the series Vibrational Spectra of Carboxylate Complexes. Parts III–VI: ref 25, 21, 27, 28.
(2) Cannon, R. D. *Electron Transfer Reactions*; Butterworths: London, 1980; Chapter 8.
(3) Catterick, J.; Thornton, P. *Adv. Inorg. Chem. Radiochem.* **1977**, *20*, 291.
(4) New, D. B. Ph.D. Thesis, Queen Mary College, London, 1975.
(5) Ponomarev, V. I.; Filipenko, O. S.; Atovmyan, L. O.; Bobkova, S. A.; Turtê, K. I. *Dok. Akad. Nauk. SSSR* **1982**, *262*, 346; *Sov. Phys. Dokl.* **1982**, *27*, 6.
(6) Oh, S. M.; Hendrickson, D. N.; Hassett, K. L.; Davis, R. E. *J. Am. Chem. Soc.* **1984**, *106*, 7984.
(7) Oh, S. M.; Kambara, T.; Hendrickson, D. N.; Sorai, M.; Kaji, K.; Woehler, S. E.; Wittebort, R. J. *J. Am. Chem. Soc.* **1985**, *107*, 5540.
(8) Oh, S. M.; Hendrickson, D. N.; Hassett, K. L.; Davis, R. E. *J. Am. Chem. Soc.* **1985**, *107*, 8009.
(9) Sorai, M.; Kaji, K.; Hendrickson, D. N.; Oh, S. M. *J. Am. Chem. Soc.* **1986**, *108*, 702.
(10) Woehler, S. E.; Wittebort, R. J.; Oh, S. M.; Hendrickson, D. N.; Inniss, D.; Strouse, C. E. *J. Am. Chem. Soc.* **1986**, *108*, 2938.
(11) Cotton, F. A.; Lewis, G. E.; Mott, G. N. *Inorg. Chem.* **1982**, *21*, 3316.
(12) Cotton, F. A.; Wang, W. *Inorg. Chem.* **1982**, *21*, 2675.
(13) Baikie, A. R. E.; Hursthouse, M. B.; New, D. B.; Thornton, P. *J. Chem. Soc., Chem. Commun.* **1978**, 62.
(14) Baikie, A. R. E.; Hursthouse, M. B.; New, L.; Thornton, P.; White, R. G. *J. Chem. Soc., Chem. Commun.* **1980**, 684.
(15) Cotton, F. A.; Norman, J. G. *Inorg. Chim. Acta* **1972**, *6*, 411.
(16) Ciechanowicz, M.; Griffith, W. P.; Pawson, D.; Skapski, A. C.; Cleare, M. J. *Chem. Commun.* **1971**, *15*, 876.
(17) Baumann, J. A.; Salmon, D. J.; Wilson, S. T.; Meyer, T. J. *Inorg. Chem.* **1979**, *18*, 2471.
(18) (a) Brown, D. B.; Robin, M. B.; McIntyre, J. D. F.; Peck, W. F. *Inorg. Chem.* **1970**, *9*, 2315. (b) Ginzburg, S. I.; Yuz'ko, M. I.; Sal'skaya, L. G. *Zh. Neorg. Khim.* **1963**, *8*, 839; *Russ. J. Inorg. Chem.* **1963**, *8*, 429. (c) Ginzburg, S. I.; Fomina, T. A.; Eistaf'eva, O. N. *Zh. Neorg. Khim.* **1974**, *19*, 1358; *Russ. J. Inorg. Chem.* **1974**, *19*, 739.
(19) Glowiak, T.; Kubiak, M.; Szymanska-Buzar, T.; Jezowska-Trzebiatowska, B. *Acta Crystallogr.* **1977**, *B33*, 3106.

0002-7863/87/1509-2009$01.50/0

Table I. Crystal Structure Data for Mixed-Valence and Mixed-Metal Oxo-Centered Trinuclear Complexes

compound	space group	site[a] symmetry	Z[b]	ref
	Mixed-Valence			
$[Mn_3O(OOCCH_3)_6(py)_3](py)_x$[c]	$R32$	D_3	3	7, 13
$[Fe_3O(OOCCH_3)_6(py)_3](py)$	$R32$[g]	D_3[g]	3	3, 4, 7, 9, 10, 13
$[Fe_3O(OOCCH_3)_6(4Et\text{-}py)_3](C_6H_6)$	$R32$	D_3	3	7, 10
$[Cr_3O(OOCCF_2H)_6(py)_3]Et_2O$	$R32$	D_3	3	12
$[Cr_3O(OOCCF_2H)_6(4CN\text{-}py)](C_6H_5CH_3)$	$P\bar{3}c$	C_3	12	12
$V_3O(OOCCF_3)_6(THF)_3$	$P2_1/m$	C_s	2	11
$[Fe_3O(OOCCH_3)_6(4Et\text{-}py)_3](4Et\text{-}py)$	$C2/c$	C_2	4	6, 8
$[Fe_3O(OOCCF_3)_6(H_2O)_3]3.5H_2O$	$A2/a$	general	8	5
$[Mn_3O(OOCCH_3)_6(3Cl\text{-}py)_3](3Cl\text{-}py)$	$P2_1/a$	general	4	8, 14
$Ru_3O(OOCCH_3)_6(P(C_6H_5)_3)_3$	$P\bar{1}$	general	2	15
$(NH_4)_4[Ir_3N(SO_4)_6(OH_2)_3]$	$I\bar{4}3d$	C_3	16	16
	Mixed-Metal			
$[Cr_2FeO(OOCCH_3)_6(OH_2)_3]NO_3CH_3COOH$	$P2_1/c$	general	4	19
$[Fe_2MO(OOCCH_3)_6(py)_3](py)$[d]	$R32$	D_3	3	22
$[Fe_2NiO(OOCCH_3)(py)_3](py)$[e]	C_c	general[f]	4	22
	$C2/c$	C_2		

[a] Site symmetry at the central oxygen atom. [b] Z = number of formula units per unit cell. [c] $x = 0$; also samples with $0 < x < 1.4$ have the same space group. [d] M = Mg, Mn, Co, Zn; $Cr^{III}_2Fe^{II}$, $Cr^{III}_2Co^{II}$, and some $Cr^{III}Fe^{III}M^{II}$ also isomorphous with these. [e] $Cr^{III}_2Mg^{II}$, $Cr^{III}_2Ni^{II}$, and $Cr^{III}Fe^{III}Ni^{II}$ analogues are also isomorphous with this complex. [f] Uncertain which of these two space groups applies. [g] Above ~190 K (ref 7).

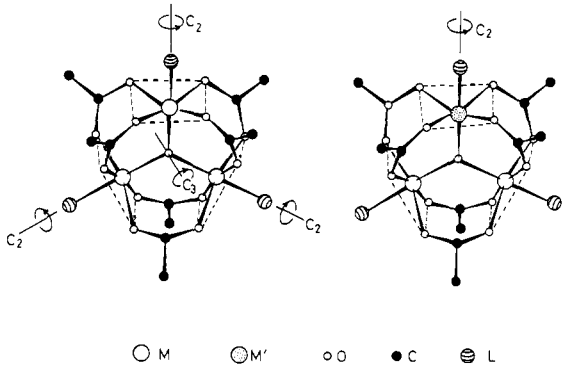

Figure 1. Framework geometry of the complexes $[M_3O(OOCR)_6L_3]$ and $[M_2M'O(OOCR)_6L_3]$.

ion is structurally distinct from the other two (C_{2v} symmetry). In the former case the outer valence electrons will be fully delocalized; in the latter case the electrons will be localized, though the extent of localization may vary, so that the effective ground-state ionic charges are $(3 - x)$, $(3 - x)$, $(2 + 2x)$, where x ranges from 0 to $^1/_3$. For any value of x between these limits there is, however, the further possibility of dynamic delocalization due to the thermally activated intramolecular electron transfer reaction:

$$M^{3-x}M^{3-x}M^{2+2x} \underset{}{\overset{k_{et}}{\rightleftharpoons}} M^{3-x}M^{2+2x}M^{3-x} \quad (1)$$

X-ray diffraction studies of the mixed-valence complexes indicate trigonal symmetry in some cases but not in others. A summary of the reported space groups and site symmetries is presented in Table I. In four cases the sites have exact threefold symmetry, C_3 or D_3, and in the earlier studies the authors concluded that the electronic configurations were of the delocalized type. On the other hand, several mixed-metal complexes also appear trigonal and are actually isomorphous with two of the mixed valence compounds. This implies rotational disordering of the mixed-metal clusters, and it suggests that the mixed-valence clusters could be localized $M^{III}_2M^{II}$ but disordered, either statically or dynamically. In other cases the mixed-valent cluster is not centred on a trigonal site, and significant bond length differences have been observed. Two of these are rigorously C_{2v}, but they deviate from trigonal symmetry in opposite ways: two metal ions with short and one with long metal–ligand bonds in the complex $[Fe_3O(OOCCH_3)_6L_3]L$ (L = 4-cyanopyridine), but two short and one long in $[V_3O(OOCCH_3)_6(py)_3]$. Moreover, some complexes have no crystallographically imposed symmetry. In two of these, all three sets of metal–ligand distances are different, but the most remarkable is $[Mn_3O(OOCCH_3)_6L_3]$ (L = 3-chloropyridine), which is very close to C_{2v}, with metal–ligand distances characteristic of two Mn^{III} ions and one Mn^{II}, while the corresponding complex with L = pyridine has all three Mn ions indistinguishable. In a recent series of papers on complexes of the type $[Fe_3O(OOCCH_3)_6L_3]S$ (S = solute molecule, e.g., C_5H_5N or C_6H_6), Hendrickson and co-workers have provided strong evidence for both static and dynamic disorder mainly affecting the groups L and S, and they have shown instances in which the rate of reaction 1 is probably controlled by the rate of the disordering process.[6-10]

All these data suggest that, in a given complex, the difference between D_{3h} and C_{2v} symmetry depends on a very fine balance of forces and can be tipped either way by crystal packing effects. Presumably, although not yet disclosed by structural studies, the central metal triangle can be distorted from equilateral, but rotationally disordered, either statically or by a dynamic pseudorotation.

Surprisingly perhaps, these ambiguities apply also to the fully oxidized M^{III}_3 complexes, at least when the metal ions are paramagnetic. Measurements of susceptibility and specific heat of Cr^{III}_3 and Fe^{III}_3 oxo-centered trimers have revealed deviations from the Heisenberg–Dirac–Van Vleck model of antiferromagnetic coupling when only one coupling constant is allowed for, and there has been a long controversy as to whether the deviations are to be explained in terms of lowering of symmetry of the metal-ion triangles, intertrimer interaction, coexistence of different trimer geometries in the same crystal structure, or a dynamic distortion again involving rapid pseudorotation of C_{2v} molecules.[20]

For all these reasons it seems imperative to try to establish the molecular symmetry by some independent technique. It is well understood that for any particular system, the result obtained will depend on the time scale of the measurement, compared with the time scale of the electron transfer. It is arguable, however, that for most purposes the vibrational time scale is the fundamental one, since it is when the rate constant k_{et} approaches the frequency ν_{et} of the molecular vibration along the reaction coordinate that the ground state geometry approaches the limiting D_{3h} symmetry. We have therefore begun a program of study of mixed-valence cluster complexes, using vibrational spectroscopy. Our method is to compare the spectra of mixed-valence complexes with those of corresponding mixed-metal complexes which are necessarily of C_{2v} symmetry. In an earlier paper,[21] a mixed-valence $Fe^{III}_2Fe^{II}$ complex was compared with mixed-metal $Fe^{III}_2Cr^{III}$ and $Fe^{III}Cr^{III}_2$ complexes, but the results were inconclusive. The important mode

(20) Jones, D. H.; Sams, J. R.; Thompson, R. C. *J. Chem. Phys.* **1984**, *81*, 440 and references cited therein.

(21) Johnson, M. K.; Cannon, R. D.; Powell, D. B. *Spectrochim. Acta* **1982**, *38A*, 307.

Table II. Infrared Bands (800–400 cm^{-1}) and Assignments[a]

Band [b] / Assignment [c] / Complex [d]	2 py mode 4	10a $\nu_{as}Fe_2MO$	3 py mode 11	4,5 δOCO	6 py mode 6b	7 py mode 6a	8 πCO_2	10 $\nu_{as}Fe_3O$	10b $\nu_{as}Fe_2MO$	11 $\rho_r CO_2$	13 py mode 16b
$[Fe_3O(OOCCH_3)_6(NC_5H_5)_3][NO_3]$	768 758	-	702 695	670 658	n.o.	639 631	615	600	-	522	440 432
$Fe_2MnO(OOCCH_3)_6(NC_5H_5)_3$	752	712	700 689	655	645	630	615	-	535	515	430
$Fe_2FeO(OOCCH_3)_6(NC_5H_5)_3$	760	obs	698	655*	655*	629	614	-	570	530	428
$Fe_2CoO(OOCCH_3)_6(NC_5H_5)_3$	755	712	705 690	655	650	632	617	-	545	530	430
$Fe_2NiO(OOCCH_3)_6(NC_5H_5)_3$	762	722	700	658*	658*	630	620	-	565	535	437
$[Fe_3O(OOCCH_3)_6(NC_5O_5)_3][NO_3]$	n.o.	-	548 540	670 658	obs	610	obs	obs	-	525	392 400
$Fe_2MnO(OOCCH_3)_6(NC_5O_5)_3$	n.o.	705	527	655	645	607	617	-	535	515	392
$Fe_2FeO(OOCCH_3)_6(NC_5O_5)_3$	n.o.	695	533 520	655*	655*	603	612	-	570	500	388
$Fe_2CoO(OOCCH_3)_6(NC_5O_5)_3$	n.o.	705	530	655	650	608	617	-	545	510	392
$Fe_3NiO(OOCCH_3)_6(NC_5O_5)_3$	n.o.	720	538	658*	658*	602	618	-	565	obs	395
$[Fe_2O(OOCCH_3)_6(OH_2)_3][NO_3]$	-	-	-	675 663	-	-	618	609	-	530	-
$Fe_2MnO(OOCCH_3)_6(OH_2)_3$	-	725	-	660	-	-	618	-	555	525	-
$Fe_2FeO(OOCCH_3)_6(OH_2)_3$	-	710	-	660	-	-	615	-	555	525	-
$Fe_2CoO(OOCCH_3)_6(OH_2)_3$	-	725	-	665	-	-	619	-	565	530	-
$Fe_2NiO(OOCCH_3)_6(OH_2)_3$	-	730	-	665	-	-	620	-	580	540	-
$Fe_2MnO(OOCCO_3)_6(OH_2)_3$	-	725	-	640	-	-	538	-	555	485	-
$Fe_2FeO(OOCCO_3)_6(OH_2)_3$	-	712	-	640	-	-	538	-	obs	485	-
$Fe_2CoO(OOCCO_3)_6(OH_2)_3$	-	720	-	635	-	-	530	-	550	480	-
$Fe_2NiO(OOCCO_3)_6(OH_2)_3$	-	726	-	640	-	-	538	-	575	490	-

[a] T = 298 K. n.o. = not observed; obs = obscure (i.e., not observed, but another band is seen at the expected frequency); * = two or more bands assumed to coincide; sh = shoulder, frequency not well defined. [b] Except for bands 10a and 10b, the numbering corresponds to ref 27. [c] See text and ref 27. The notation for the pyridine modes is that of ref 37–39. [d] The complexes contain various numbers of pyridine or H_2O molecules, as noted in the text.

$\nu_{as}(M_2M'O)$ (see below) was obscured in some of the spectra, hence most attention was paid to the low-frequency range 400–150 cm^{-1}, where, it now turns out, the diagnostically useful band 15a (see below) is resolved only at low temperatures. Subsequently, through the work of Blake and co-workers,[22] the mixed-metal complexes $[Fe^{III}_2M^{II}O(OOCCH_3)_6L_3]$, with M = Mn, Co, Ni, etc., have become available, and we have found these to be a much more useful basis of comparison. We now report results which show clearly that the mixed-valence iron complexes are of the localized C_{2v} type, though the valence localization is apparently not so complete as in the mixed-metal species.

Experimental Section

Preparation of Complexes. Tri(aquo)hexakis(μ-acetato)(μ_3-oxo)triiron(III,III,II) was prepared by an improvement of the original method.[23] A solution of $FeCl_2{\cdot}4H_2O$ (5 g, 25 mmol), CH_3COONa (5 g, 60 mmol), and glacial CH_3COOH (20 mL) in 70 mL of water was allowed to stand in a 500-mL beaker covered with a watch glass for 5 days at room temperature. The black crystalline product was washed with ethanol, dried in vacuo, and stored under nitrogen. Anal. Calcd for $[Fe_3O(OOCCH_3)_6(OH_2)_3]$: C, 24.32; H, 4.05; Fe^{II}, 9.46; Fe(total), 28.34. Found: C, 24.23; H, 4.39; Fe^{II}, 7.27; Fe(total), 28.24.

The pyridine adduct $[Fe_3O(OOCCH_3)_6(py)_3]0.5py$ was prepared by the literature method,[24] and the deuteriopyridine and γ-picoline analogues were prepared similarly.

Tri(aquo)hexakis(μ-acetato)(μ_3-oxo)triiron(III) nitrate, $[Fe_3O(OOCCH_3)_6(OH_2)_3]NO_3{\cdot}3H_2O$, and the pyridine adduct, $[Fe_3O(OOCCH_3)_6(NC_5H_5)_3]NO_3$, were prepared as before.[25]

Mixed-Metal Complexes. Following Blake et al.[22a,c] these were prepared by the methods of Weinland and Holtmeier.[26] The earlier authors formulated the compounds as $M^{II}_4[Fe^{III}_9(OH)_9(OOCCH_3)_{26}]{\cdot}23H_2O$ and $M^{II}_3[Fe^{III}_6O_3(OH)(OOCCH_3)_{17}]12py$, but Blake et al. have shown that they all have the triangular $Fe^{III}_2M^{II}$ structure. Elemental analysis (C, H, N, Fe) confirmed the formulae $[Fe_2MO(OOCCH_3)_6(OH_2)_3]xH_2O$ with x = 2 to 3 and $[Fe_2MO(OOCCH_3)_6(py)_3]xpy$ with x = 0.5 (M = Mn) and 1.0 (M = Co, Ni). Infrared spectra agreed with samples supplied by Dr. Blake in all cases. Deuteriated and γ-picoline derivatives were prepared in the same way.

Spectra. Infrared spectra in the region 800–400 cm^{-1} were recorded on a Perkin-Elmer 684 ratio recording spectrophotometer, using KBr or CsI disks, and in the region 400–130 cm^{-1} on a Beckman RIIC IR7204 Fourier interferometer, using Nujol mulls on polyethylene disks. Reproducibility, checked with the sharpest available peaks, was ±1 cm^{-1}.

Raman spectra were recorded on a Spex 1401 double-monochromator laser Raman instrument, with Spectra Physics type 165 ion laser sources. A rotating sample cell was used, the material being pressed into a circular groove, under ca. 4–5 tons of pressure. The rotation speed is about 3000 rpm. For smaller samples a layer of KBr was first pressed onto the cell and the sample was sprinkled thinly on the surface and pressed again.

Symmetry Considerations. The molecular structures of the homonuclear Fe^{III}_3 and mixed $Fe^{III}_2M^{II}$ carboxylate complexes are shown in Figure 1. Neglecting complications due to crystal site symmetry, these are of D_{3h} and C_{2v} symmetry, respectively, but we have found that most features of the spectra can be interpreted in terms of smaller moieties within the molecules and that most though not all of the possible coupling effects can be neglected. Internal vibrations of the pyridine molecules and carboxylate anions are similar to those in other related complexes. As regards the metal–ligand framework, in previous studies of the homonuclear complexes this was successfully treated as three planar MO_4 units, locally D_{4h}, interacting under D_{3h} molecular symmetry.[25] More precisely, however, the three units are MLO_5, locally C_{4v}; and taking into account the whole molecule, the symmetry of an individual metal site is C_{2v}. Correlations between all these relevant symmetries are shown in Figure 2.

(22) (a) Blake, A. B.; Yavari, A.; Kubicki, H. *J. Chem. Soc., Chem. Commun.* **1981**, 796. (b) Blake, A. B.; Yavari, A. *J. Chem. Soc., Chem. Commun.* **1982**, 1247. (c) Blake, A. B.; Yavari, A.; Hatfield, W. E.; Sethulekshmi, C. N. *J. Chem. Soc., Dalton Trans.* **1985**, 2509.

(23) Chrētien, A.; Lous, P. *Bull. Soc. Chim. Fr.* **1944**, *11*, 446.

(24) Dziobkowski, C. T.; Wrobleski, J. T.; Brown, D. B. *Inorg. Chem.* **1981**, *20*, 679.

(25) Johnson, M. K.; Powell, D. B.; Cannon, R. D. *Spectrochim. Acta* **1981**, *37A*, 995.

(26) Weinland, R. F.; Holtmeier, H. *Z. Anorg. Allge. Chem.* **1928**, *173*, 49.

Table III. Infrared Bands (400–130 cm^{-1})[a]

Band[b]	15, 15a		16	16a, 16b	17	17a	18, 18a		17b	17c	19	20
Assignment[c]	MO_4		$\delta_s M_3O$	-	$\nu_{as}FeN$	-	MO_4		νMN	νMN	-	-
Complex[d]												
$[Fe_3O(OOCCH_3)_6(NC_5H_5)_3][NO_3]$	360	–	297	-	253*	253*	233		-	-	210	190
$Fe_2MnO(OOCCH_3)_6(NC_5H_5)_3$	328	305	274	281, obs	-	251	218*,	218*	218*	180	158	130
$Fe_2FeO(OOCCH_3)_6(NC_5H_5)_3$	330	308	274	281, 265	-	250	224,	?205	obs	186	156	135
$Fe_2CoO(OOCCH_3)_6(NC_5H_5)_3$	332	310	278	285, 265	-	248	233,	obs, 208	c.218	192, 186	165	134
$Fe_2NiO(OOCCH_3)_6(NC_5H_5)_3$	338	317	283	289, 270	-	253*	253*,	228, 221	obs	215, 206	169	144
$Fe_2MnO(OOCCH_3)_6(NC_5O_5)_3$	327	306	282	275, obs	-	252	218,	obs	209	178	160	130
$Fe_2FeO(OOCCH_3)_6(NC_5O_5)_3$	328	308	280	274, obs	-	249	223,	obs	214	184	n.o.	n.o.
$Fe_2CoO(OOCCH_3)_6(NC_5O_5)_3$	330	309	285	278, 264	-	247	233,	obs	214	188	165	135
$Fe_2NiO(OOCCH_3)_6(NC_5O_5)_3$	338	317	289	282, 269	-	253*	253*,	229 221	n.o.	214, 207	170	~140
$Fe_2MnO(OOCCH_3)_6(NC_5H_4Me\text{-}4)_3$	332	308	282	274, 265	-	248	225,	207	202	174	156	n.o.
$Fe_2FeO(OOCCH_3)_6(NC_5H_4Me\text{-}4)_3$	332	310	276*	276*, 264	-	251	226*,	226*	208	180	n.o.	n.o.
$Fe_2CoO(OOCCH_3)_6(NC_5H_4Me\text{-}4)_3$	332	310	287	278, 264	-	253	234,	209*	209*	190	n.o.	130
$Fe_2NiO(OOCCH_3)_6(NC_5H_4Me\text{-}4)_3$	334	317	292	285, 271	-	252*	252*,	212	?237	obs, 199	170	n.o.
$[Fe_3O(OOCCH_3)_6(OH_2)_3][NO_3]$	364	-	304	-	-	240	224		-	-	200	185
$Fe_2MnO(OOCCH_3)_6(OH_2)_3$	325	sh	280	264	-	248	226,	200	-	-	180	~150
$Fe_2FeO(OOCCH_3)_6(OH_2)_3$	330	sh	282	268	-	247	226,	211	-	-	obs	~155
$Fe_2CoO(OOCCH_3)_6(OH_2)_3$	330	sh	284	n.o.	-	250	226*,	226*	-	-	obs	~160
$Fe_2NiO(OOCCH_3)_6(OH_2)_3$	338	sh	288	270	-	251*	251*,	?225	-	-	203	~162
$Fe_2MnO(OOCCO_3)_6(OH_2)_3$[e]	325	-	278	260	-	236	obs,	186	-	-	165	~135
$Fe_2FeO(OOCCO_3)_6(OH_2)_3$[e]	326	-	278	260	-	235	obs,	200	-	-	obs	~140
$Fe_2CoO(OOCCO_3)_6(OH_2)_3$[e]	326	-	282	260	-	236	217,	204	-	-	obs	~145
$Fe_2NiO(OOCCO_3)_6(OH_2)_3$[e]	330	-	284	263	-	238*	238*,	203	-	-	172	~153

[a] T = 77 K. See also Table I, footnote *a*. [b] Bands 15, 16, 17, 18, 19, 20 are numbered to correspond with ref 27. [c] See text, M = Fe^{III} or divalent metal. [d] The complexes contain various numbers of pyridine, 4-methylpyridine, or water molecules, as noted in the text. [e] Room temperature.

Band Assignments, 800–400 cm^{-1}. Infrared spectra of the mixed complexes $[Fe^{III}_2M^{II}O(OOCCH_3)_6L_3]$ with L = C_5H_5N, C_5D_5N, and H_2O and M = Mn, Fe, Co, and Ni are displayed in Figure 3. Band frequencies and assignments are listged in Table II. As before,[27] bands 2, 3, 6, 7, and 13 have been assigned to modes of the coordinated pyridine molecules, on the basis of comparisons with the free ligand and deuteriation shifts. Two other strong bands common to all the spectra have been assigned to deformations of the CO_2 units (bands 5 and 8), confirmed in the aquo complexes by shifts when CH_3COO^- is replaced by CD_3COO^-. A third, weaker band, which also shifts with deuteriation, is provisionally assigned to the in-plane CO_2 deformation (band 11).

In the complex $[Fe^{III}_3O(OOCCH_3)_6(NC_5H_5)_3]^+$, the asymmetric in-plane vibration of the central oxygen has been assigned[27] to the shoulder at 600 cm^{-1} on the basis of the substantial shift on replacement with ^{18}O. Only one band in the frequency range under consideration shows such a shift, as expected under D_{3h} molecular symmetry. In the mixed-metal complexes, however, when all the above-mentioned bands are discounted, we find in general two bands which show no appreciable shift on deuteriation of the pyridine or the acetate groups, and these are assigned to the split components of the in-plane vibration due to the reduction in symmetry from D_{3h} to C_{2v} (Figure 2). The assignment has been confirmed by the ^{18}O shift in the complex $[Fe^{III}_2Ni^{II}O(OOCCH_3)_6(NC_5H_5)_3]$.[28] The two bands are particularly clear in the deuteriopyridine adducts (Figure 3, bands 10a and 10b). In the pyridine series, the lower-frequency band 10b is also clear, but the higher-frequency band overlaps with the pyridine band 3 in some complexes. In the aquo complexes both bands are clearly resolved. Viewing the mixed-valence complexes $[Fe_3O(OOCCH_3)_6L_3]$ in relation to these, we observe the corresponding bands 10a and 10b in the two complexes, L = H_2O and C_5D_5N; but they are noticeably broader and less intense than in the mixed-metal series. In the pyridine adduct, L = C_5H_5N, band 10a is again evidently obscured by band 3.

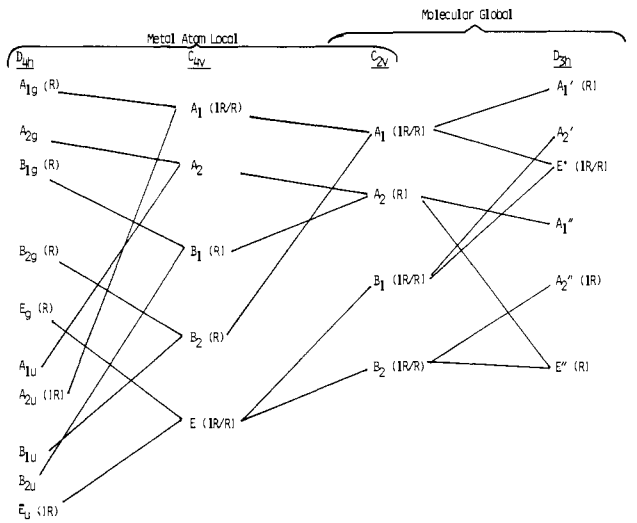

Figure 2. Correlation of symmetries of normal vibrations under various local and molecular symmetries in $[M_2M'O(OOCCH_3)_6L_3]$ complexes.

Raman spectra of the complexes $[Fe^{III}_2M^{II}O(OOCCH_3)_6(OH_2)_3]$, M = Mn, Fe, Co, and Ni, are shown in Figure 4. Bands 10a, 5, 8, 10b, and 11 are all reasonably well marked and correspond to the infrared frequencies within ±5 cm^{-1}.

Band Assignments, 400–130 cm^{-1}. Infrared spectra in the region 400–130 cm^{-1} are shown in Figure 5. Band frequencies and assignments are listed in Table III. The vibrations expected in this region are metal–acetate and metal–pyridine stretching and deformation, out-of-plane deformation of the central oxygen atom, and lattice modes below about 150 cm^{-1}. Considering the large size of the molecules, and the multiple unit cell occupancy (Table I), a large number of modes must

(27) Montri, L.; Cannon, R. D. *Spectrochim. Acta* **1985**, *41A*, 643.
(28) Meesuk, L.; Jayasooriya, U. A.; Cannon, R. D. *Spectrochim. Acta*, in press.

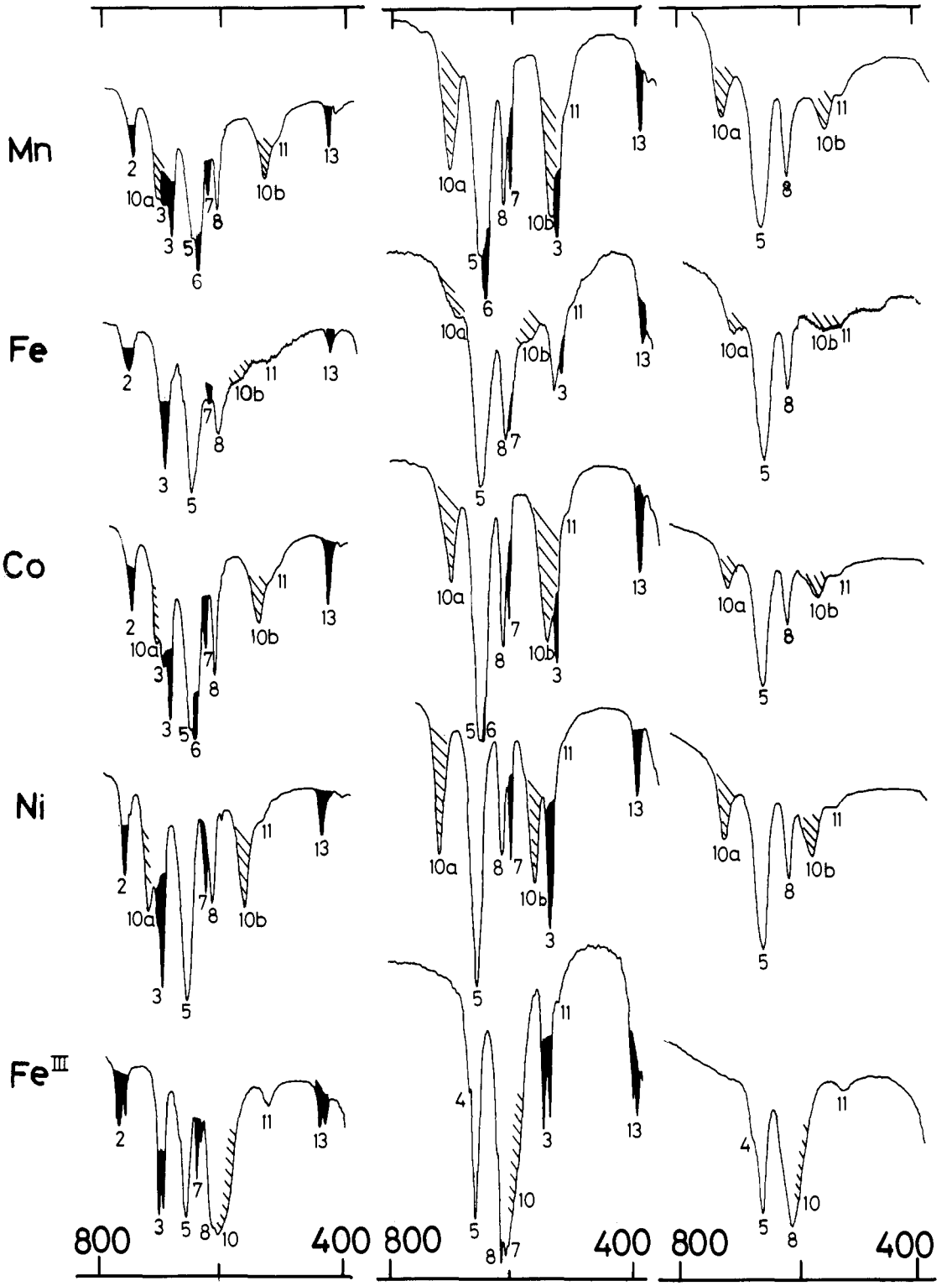

Figure 3. Infrared spectra of complexes $[Fe^{III}_2M^{II}O(OOCCH_3)_6L_3]$ and $[Fe^{III}_3O(OOCCH_3)_6L_3][NO_3]$. Left-hand series L = C_5H_5N; middle, L = C_5D_5N; right, L = H_2O. Room temperature.

occur close together in this frequency range, and mixing of modes is therefore expected. Nevertheless, we find that an isolated-molecule approach provides a reasonable explanation of the available data.

Considering the square-planar MO_4 units, there are only three fundamentals which are infrared active under D_{4h} symmetry. In Herzberg's notation[29] these are the doubly degenerate stretch and deformation, $\nu_6(E_u)$ and $\nu_7(E_u)$, respectively, and the out-of-plane deformation, $\nu_3(A_{2u})$. From the correlation diagram (Figure 2), it is clear that these modes retain their infrared activity right across all symmetries, and therefore it is reasonable to expect them to be the most prominent of the MO_4 vibrations. The highest-frequency band in this region is also the most intense (Figure 5, band 15), hence it is assigned to have its parentage in the local $\nu_6(E_u)$ mode. Its breadth, which is notable in the Fe^{III}_3 complexes as well as in the mixed-metal complexes, is probably an indication of splitting under the more realistic local symmetry C_{2v}. In the mixed-metal and mixed-valent complexes, however, this band is further split into two distinct peaks (15 and 15a), with an approximate intensity ratio 2:1, and this agrees with the presence of the two types of metal center in the molecule. Band 18 shows similar behavior to band 15, through not so clearly owing to overlap with other bands, and is taken to originate from $\nu_7(E_u)$. The out-of-plane deformation $\nu_3(A_{2u})$ is expected to be at lower frequency and is not assigned. All these bands shift somewhat on deu-

(29) Herzerg, G. *Molecular Spectra and Molecular Structure*; Van Nostrand: Princeton, 1945; Vol. II.

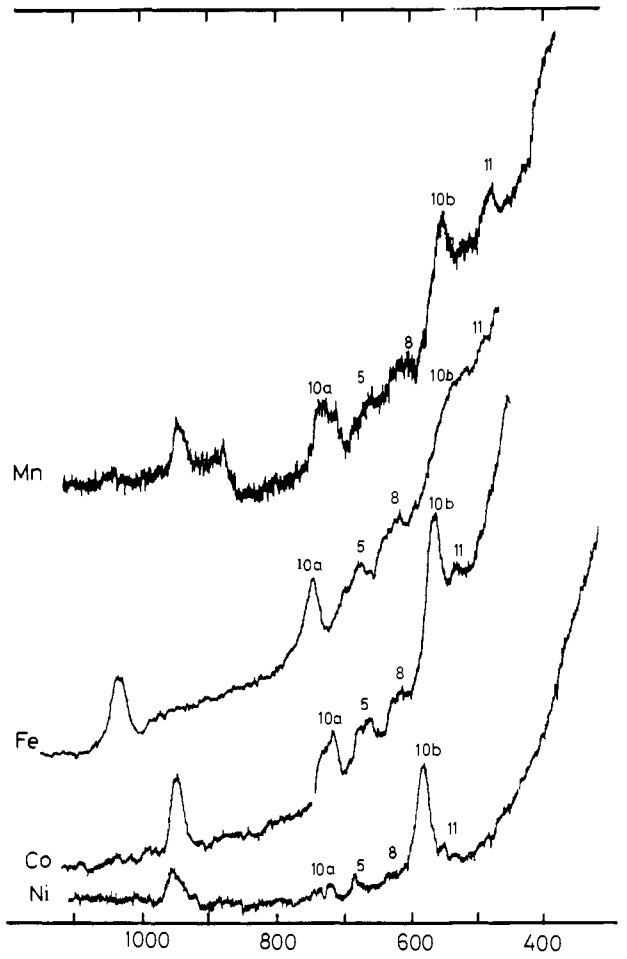

Figure 4. Raman spectra of complexes $[Fe^{III}_2M^{II}O(OOCCH_3)_6(OH_2)_3]$, M = Mn, Fe, Co, and Ni. Room temperature; exciting line 5145 Å.

teration of the acetate groups (Table III), and they increase regularly in frequency according to the hetero-metal ion, Mn < Fe < Co < Ni < Fe^{III}, as expected for metal–oxygen stretches.

The strong band 17a differs from these. It is more sensitive to deuteriation but much less sensitive to change of metal M or ligand L. Thus it does not seem to be a metal–oxygen stretch (nor $\delta_s(Fe_2MO)$ as suggested by Oh et al.[7]). It is therefore assigned to a skeletal mode, which involves mainly an out-of-plane deformation of the methyl groups. In the (Fe^{III}_3)pyridine adduct, a band at similar frequency to these bands does show sensitivity to ligand L, and it has been assigned to an Fe–N stretch.[21] The skeletal deformation is presumably overlapped by this mode.

In the triiron(III) pyridine adducts, band 16 (Figure 5) has been reliably identified as the out-of-plane deformation of the central oxygen, on the basis of ^{18}O isotopic substitution.[27] The mixed-metal and mixed-valent compounds show a group of up to three bands in this region with mainly ^{18}O- and deuterium-substitution sensitivity.[28] Evidently these involve the out-of-plane oxygen deformation, together with other modes of the same symmetry which can couple with it. For example, they could be MO_4 stretches, which would be forbidden in strict D_{4h} symmetry, but which gain appreciable intensity when the symmetry is strongly lowered by the effect of the mixed metals, or, more likely, rotation of the MO_4 units about the lines of intersection of the MO_4 and Fe_2M planes. In Figure 6 and Table III, these bands are labeled I6 (to denote π-Fe_2MO) and 16a and I6b, but they are not assumed to be pure modes,[28] and both the correlations and the assignment are provisional.

In the pyridine and γ-picoline adducts, further strong bands occur as shown in Figure 7, and these are assigned to the metal–nitrogen stretches. They occur in the range 175–240 cm^{-1}, which is similar to the range of metal–pyridine stretches in the complexes $[M^{II}(py)_4(NCS)_2]$.[30] Bands 17c of the Fe_2Fe^{II} and Fe_2Co^{II} complexes shift slightly with deuteriopyridine, and further with γ-picoline, and the same is true of two bands marked 17c for the Fe_2Ni^{II} complex. The shifts are similar to those previously reported: for deuteriopyridine 2 to 3 cm^{-1}, as compared to 1

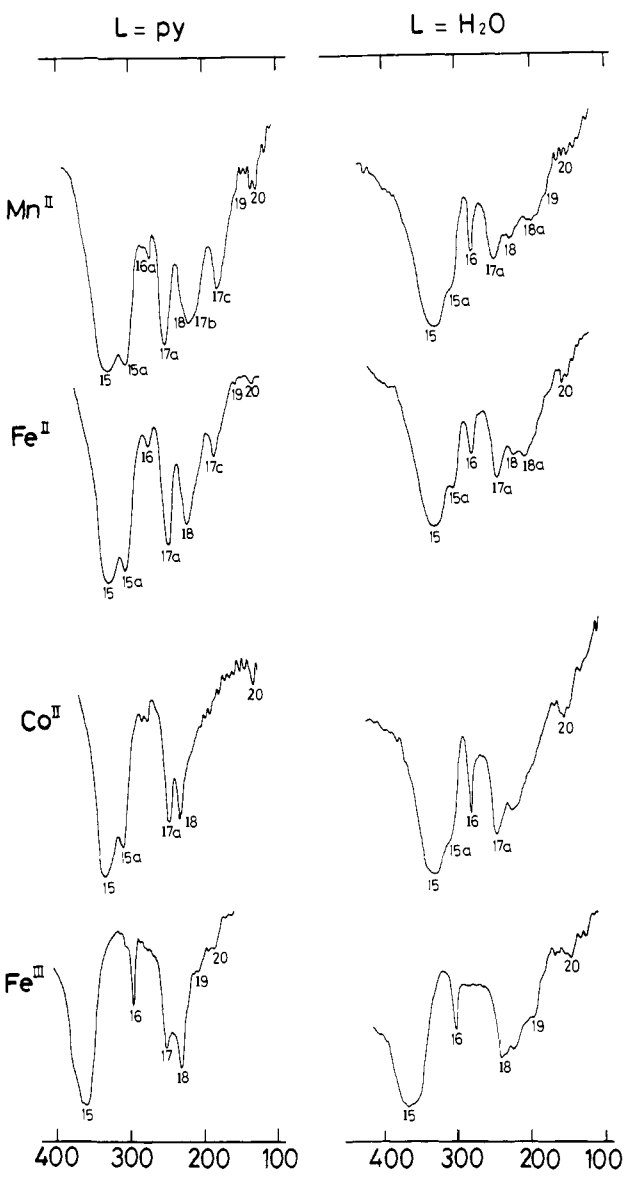

Figure 5. Low-frequency infrared spectra of complexes $[Fe^{III}_2M^{II}O(OOCCH_3)_6L_3]$ (M = Mn, Fe, and Co) and $[Fe^{III}_3O(OOCCH_3)_6L_3][NO_3]$. Left-hand side, L = C_5H_5N; right-hand side, L = H_2O. T = 77 K.

to 4 cm^{-1} in $[M^{II}(py)_4(NCS)_2]$;[30] and for γ-picoline 7 to 12 cm^{-1}, compared with 5 to 12 cm^{-1} in symmetrical trivalent metal complexes of the present type.[25] We regard the bands 17c as a correlated sequence with a small splitting which increases from Mn to Ni. The sequence 17b is equally clear for the Mn, Fe, and Co complexes. The band is not resolved in the pyridine adduct, but it is seen in the deuteriopyridine adducts and shifts further with γ-picoline. The corresponding band of Fe_2Ni^{II} cannot be seen. It is expected in the range 235–245 cm^{-1}. Further, provisional, assignments in this region are listed in Table III.

Discussion

It seems clear that bands 10a and 10b are to be assigned to the B_2 and A_1 components, respectively, of the in-plane vibration of the central oxygen. The A_1 component is expected to have more the character of an M^{II}–O stretch than of Fe^{III}–O, and the B_2 component conversely (see sketches in Figure 8), hence we assign the A_1 component as the lower frequency of the two. This assignment is supported by the variation of frequency with metal M. In the mixed-metal sequence, both components increase in frequency in the order Mn < Co < Ni, parallel to the Irving–Williams series of stabilities of metal–ligand complexes, and also parallel to frequency trends in other metal–pyridine complexes;[30–32]

(30) Engelter, C.; Thornton, D. A. *J. Mol. Struct.* **1977**, *42*, 51.

(31) Clark, R. J. H.; Williams, C. S. *Inorg. Chem.* **1965**, *4*, 350.

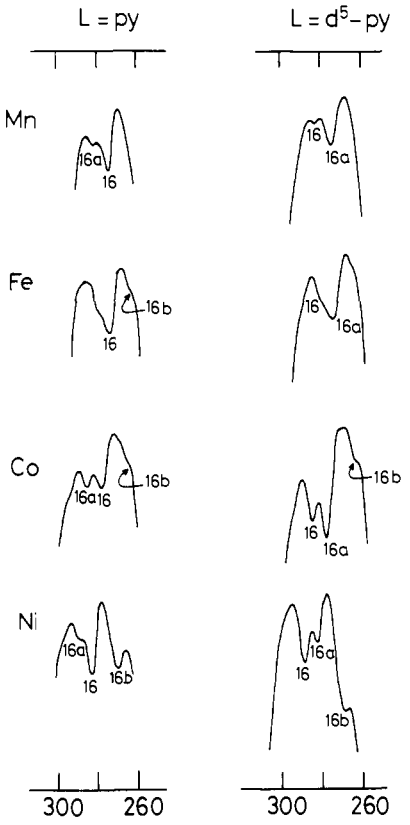

Figure 6. Infrared spectra of complexes $[Fe^{III}_2MO(OOCCH_3)_6L_3]$. Left-hand side, L = C_5H_5N(py); righth-hand side, L = C_5D_5N (d^5-py). T = 77 K.

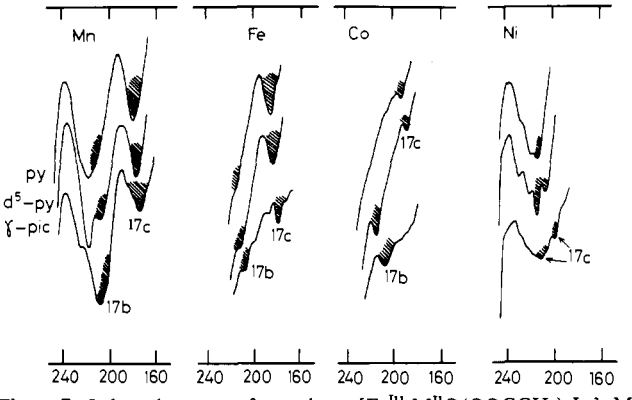

Figure 7. Infrared spectra of complexes $[Fe^{III}_2M^{II}O(OOCCH_3)_6L_3]$, M = Mn, Fe, Co, and Ni. In each group of three curves reading downwards, L = C_5H_5N (py), C_5D_5N (d^5-py), 4-$CH_3C_5H_4N$ (γ-pic). The shaded parts indicate the M–N stretch frequencies (cf. Table III). T = 77 K.

but for the A_1 mode the variation is more pronounced, again reflecting the M^{II}–O stretch character (Figure 8). The two frequencies are similar to those reported by Lippard and co-workers for analogous vibrations of binuclear iron(III) complexes. For example, in the complex $[Fe^{III}_2O(OOCCH_3)_2(TACN)_2]^{2+}$ (TACN = 1,4,7-triazacyclononane) which contains the (μ-oxo)bis(μ-carboxylato) core structure, infrared bands at 540 and 749 cm^{-1} have been assigned to the symmetric and asymmetric OFeO stretches, which are the analogues of our A_1 and B_2 modes;[33] and in an analogous complex with aminocarboxylate bridging groups (aspartate and glutamate), similar bands were found at 528 and 751 cm^{-1}, and also the deformation modes at 278 cm^{-1}

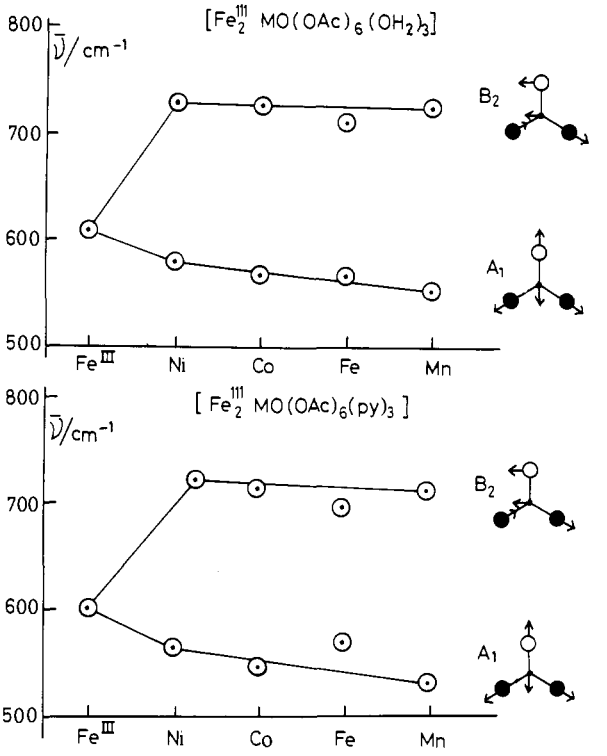

Figure 8. Correlation of frequencies of the in-plane asymmetric Fe_2MO stretch of complexes $[Fe^{III}_2MO(OOCCH_3)_6L_3]$, L = H_2O and C_5H_5N. On the horizontal axes, Fe^{III} denotes the symmetrical Fe^{III}_3O complex, and the frequency plotted is that of the degenerate E′ mode (Table II, band 10); for the other complexes the frequencies of the B_2 and A_1 (bands 10a and 10b) modes are plotted (cf. sketches at right).

corresponding to our $\pi(Fe_2MO)$.[34]

The intensities of the Raman bands further support the assignments. In the mixed-metal complexes, the A_1 mode is stronger than the B_2 mode (Figure 4), and in the iron(III) dimer, using the same exciting line, the symmetric mode is stronger than the asymmetric.[34] In the mixed-valence iron complex, the intensities are reversed (Figure 4). In all the trimeric complexes the differences are presumably due to resonance enhancement, as Lippard and co-workers have shown in detail for the dimers.[34]

In the low-frequency range the mixed-valence complexes closely resemble the mixed-metal, and differ considerably from the fully oxidized triiron(III) analogue (Figure 5). Thus, even without detailed assignments the lowering of symmetry of the mixed-valence cluster can be seen. Specifically, however, the splitting of band 15 is attributed to the nonequivalence of the Fe^{II} and Fe^{III} ions.

The Fe^{III}–L and M^{II}–L stretching frequencies are expected to show the same symmetry relationships as the in-plane central oxygen vibrations (see Figure 2). That is, for symmetrical D_{3h} complexes $[M_3O(OOCR)_6L_3]^{n+}$ we expect symmetric A_1', in the Raman only, and asymmetric E′, in the infrared and Raman. For mixed complexes $[M_2M'O(OOCR)_6L_3]^{n+}$, the A_1' mode becomes A_1, infrared and Raman active, but probably weak in the infrared; and the degeneracy of the E′ mode is lifted to produce A_1 and B_2, again both infrared and Raman active. We cannot yet test these predictions for the aquo complexes, since the location of $\nu(M–OH_2)$ is still not certain, but for the pyridine adducts $[Fe^{III}_3O(OOCCH_3)_6(NC_5H_5)_3]^+$ and $[Cr^{III}_3O(OOCCH_3)_6(NC_5H_5)_3]^+$ both components of ν(M–N) have been observed. In the case of the iron complex ν_s(Fe–N) was found in the Raman at 215 cm^{-1}, and ν_{as}(Fe–N) in the infrared at 249 cm^{-1}.[25,27] In this work, two metal–nitrogen stretches have been found, but a careful search for any other bands was inconclusive except for a small shift in band 17a, observed in the Fe_2Mn and Fe_2Ni

(32) Akyüz, S.; Dempster, A. B.; Davies, J. E. D.; Holmes, K. T. *J. Chem. Soc., Dalton Trans.* **1976**, 1746.
(33) Spool, A.; Williams, I. D.; Lippard, S. J. *Inorg. Chem.* **1985**, *24*, 2156.
(34) Armstrong, W. H.; Spool, A.; Papaefthymiou, G. C.; Frankel, R. B.; Lippard, S. J. *J. Am. Chem. Soc.* **1984**, *106*, 3653.

picoline adducts only. This could indicate that as in the case of the Fe^{III}_3 complex, there is a ν(M-N) band close to 250 cm^{-1}, overlaid by the strong and broad band 17a. What is clear, however, is that in at least three of the complexes studied here there are at least two infrared-active M-N stretches, and this includes the mixed-valence iron(III,III,II) complexes: again confirming that the symmetry is lower than D_{3h}.

There are several indications that although the symmetry of the mixed-valence iron complexes is consistent with unequal oxidation states, the localization of charges is not so clear-cut as in the mixed-metal species. As shown in Figure 8 the frequencies of the two components of ν_{as} ($Fe^{III}_2Fe^{II}O$) are out of line with the other complexes, the higher-frequency component being significantly low and the lower frequency component significantly high. Also, the actual bands are broader and less intense in the iron(II) complexes than in the others (Figure 3), and both of these anomalies are greater for the pyridine adduct than for the aquo adduct. Evidently there is some delocalization of the valences, and as pointed out above, this could be either static, or dynamic, or both. From a comparison of electronic spectra and electrochemical data, it has already been argued that static delocalization does occur, and more so in the pyridine than in the aquo adduct.[35]

This would affect the infrared spectra by lessening the difference between Fe^{III}-O and Fe^{II}-O stretching force constants. Dynamic delocalization has also been proposed on the basis of Mössbauer line broadening measurements.[6,7,24,36] The Mössbauer time scale is much slower than the infrared, but the most recent estimate of k_{et}, for the complex with L = 4-ethylpyridine, extrapolated to room temperature, is 9×10^9 s^{-1}.[6] The half-widths of our observed bands 10a and 10b are approximately 10 cm^{-1}, or in terms of frequency about 10^{11} s^{-1}. The possibility of lifetime broadening through the electron transfer reaction 1 cannot therefore be ruled out.

Acknowledgment. We thank Dr. A. B. Blake for samples of mixed-metal complexes and Dr. D. B. Powell for advice and discussion. L.M. thanks the University of East Anglia and the CVCP for financial support.

(35) Cannon, R. D.; Montri, L.; Brown, D. B.; Marshall, K. M.; Elliott, C. M. *J. Am. Chem. Soc.* **1984**, *106*, 2591.

(36) (a) Gol'danskii, V. I.; Alekseev, V. P.; Stukan, R. A.; Turtâ, K. I.; Ablov, A. V. *Dokl. Akad. Nauk SSSR* **1973**, *213*, 867; *Dokl. Phys. Chem.* **1973**, *213*, 1063; (b) *Fiz. Mat. Metody Koord. Khim., Tezisy Dokl., Vses. Soveshch. 5th* **1974**, 127. Shtiintsa, Kishinev, USSR, 1974; CA 83 35258f.

(37) Wilmshurst, J. K.; Bernstein, H. J. *Can. J. Chem.* **1957**, *35*, 1183.

(38) Green, J. H. S.; Kynaston, W.; Paisley, H. M. *Spectrochim. Acta* **1963**, *19*, 549.

(39) Long, D. A.; George, W. O. *Spectrochim. Acta* **1963**, *19*, 1777.

The Anisotropy of Intermolecular Interactions, Band Electronic Structure, and Electrical Properties of β-$(ET)_2AuCl_2$

T. J. Emge,[†] H. H. Wang,[†] M. K. Bowman,[†] C. M. Pipan,[†] K. D. Carlson,[†] M. A. Beno,[†] L. N. Hall,[†] B. A. Anderson,[†] J. M. Williams,*[†] and M.-H. Whangbo*[‡]

Contribution from the Chemistry and Materials Science Divisions, Argonne National Laboratory, Argonne, Illinois 60439, and Department of Chemistry, North Carolina State University, Raleigh, North Carolina 27695-8204. *Received September 9, 1986*

Abstract: A new organic salt, β-$(ET)_2AuCl_2$, was synthesized, and its structure and physical properties were determined. Here ET refers to bis(ethylenedithio)tetrathiafulvalene (BEDT-TTF or ET). β-$(ET)_2AuCl_2$ is isostructural with β-$(ET)_2ICl_2$ and contains the shortest anion, $AuCl_2^-$, among the β-$(ET)_2X$ salts with linear anions, X^-, known so far. Crystal data for β-$(ET)_2AuCl_2$ are as follows: triclinic, $P\bar{1}$, 298 K/120 K, a = 6.651 (1)/6.627 (2) Å, b = 9.761 (2)/9.595 (3) Å, c = 12.734 (3)/12.662 (4) Å, α = 86.12 (2)/85.15 (2)°, β = 100.70 (2)/101.40 (2)°, γ = 99.41 (2)/98.24 (2)°, and V_c = 800.7 (4)/779.8 (5) Å^3. The electrical conductivities of type I β-$(ET)_2X$ salts (i.e., those with short anions X^- = $AuCl_2^-$, ICl_2^-) measured by the four-probe technique show that they are semiconductors with thermal activation energy of 0.10 eV. The valence band (i.e., the highest occupied band) of β-$(ET)_2AuCl_2$, which is half-filled, is calculated to be one-dimensional in character as in the case of β-$(ET)_2ICl_2$. ESR data of β-$(ET)_2AuCl_2$ reveal the presence of a phase transition at ~33 K, which is somewhat higher than the corresponding temperature (22 K) of β-$(ET)_2ICl_2$. The ET molecule pairs of type I β-$(ET)_2X$ salts are significantly more dimerized than those of type II β-$(ET)_2X$ salts (i.e., those with long anions X^- = IBr_2^-, AuI_2^-, I_3^-). Short S···S contacts within the ET molecule networks of both type I and type II β-$(ET)_2X$ salts are found to decrease as the length of the anion X^- decreases. This orginates from close-packing of ET molecules around the anions X^- in the β-$(ET)_2X$ salts. For type I β-$(ET)_2X$ salts with small anions X^-, this close-packing is achieved when dimerized ET molecule pairs protrude out of their donor networks.

For the isostructural β-$(ET)_2X$ series of synthetic metals and superconductors, where X^- is a linear triatomic anion such as I_3^-,[1-3] I_2Br^-,[4,5] AuI_2^-,[6,7] IBr_2^-,[8,9] or ICl_2^-,[10] correlations between anion length and the physical properties of their salts have been developed.[5,10-12] Band electronic structure calculations[13,14] on β-$(ET)_2X$ synthetic metals show that their electrical properties are directly related to the magnitudes of donor-donor interactions within the layered networks of ET molecules. Depending on the nature of donor-donor interactions, the ET molecule layer exhibits either a two-dimensional[13,14] (2D) or a quasi-one-dimensional[10] (1D) electronic behavior. For linear anions, the intermolecular S···S contacts within the 2D ET networks of the isostructural β-$(ET)_2X$ salts generally expand as the anion length is increased,[5,11]

* Authors to whom correspondence should be addressed.
† Argonne National Laboratory.
‡ North Carolina State University.

(1) Yagubskii, E. B.; Shchegolev, I. F.; Laukhin, V. N.; Kononovich, P. A.; Kartsovnik, M. V.; Zvarykina, A. V.; Buravov, L. I. *JETP Lett.* **1984**, *39*, 12.

(2) Crabtree, G. W.; Carlson, K. D.; Hall, L. N.; Copps, P. T.; Wang, H. H.; Emge, T. J.; Beno, M. A.; Williams, J. M. *Phys. Rev. B: Condens. Matter* **1984**, *30*, 2958.

(3) Williams, J. M.; Emge, T. J.; Wang, H. H.; Beno, M. A.; Copps, P. T.; Hall, L. N.; Carlson, K. D.; Crabtree, G. W. *Inorg. Chem.* **1984**, *23*, 2558.

(4) Emge, T. J.; Wang, H. H.; Beno, M. A.; Leung, P. C. W.; Firestone, M. A.; Jenkins, H. C.; Cook, J. D.; Carlson, K. D.; Williams, J. M.; Venturini, E. L.; Azevedo, L. J.; Schirber, J. E. *Inorg. Chem.* **1985**, *24*, 1736.

(5) Emge, T. J.; Leung, P. C. W.; Beno, M. A.; Wang, H. H.; Firestone, M. A.; Webb, K. S.; Carlson, K. D.; Williams, J. M.; Venturini, E. L.; Azevdeo, L. J.; Schirber, J. E. *Mol. Cryst. Liq. Cryst.* **1986**, *132*, 363.

0002-7863/87/1509-2016$01.50/0